Dynamic Equivalent Based on Balanced Realizations for Interconnection of Photovoltaic Distributed System

Orozco, Michael; De Jesus Chavez, Jose; Popov, Marjan; Garcia-Vite, Pedro M.

DOI
10.1109/ISGTEurope.2018.8571603

Publication date
2018

Document Version
Final published version

Published in
Proceedings - 2018 IEEE PES Innovative Smart Grid Technologies Conference Europe, ISGT-Europe 2018

Dynamic Equivalent Based on Balanced Realizations for interconnection of Photovoltaic Distributed System

Michael Orozco
PGIIE-TECNM/Instituto Tecnológico de Morelia,
Morelia, Mexico
m.j.orozco@hotmail.com

Jose de Jesus Chavez,
Marjan Popov
IEPG Intelligent Electrical Power Grids
TUDELFT
Delft, the Netherlands
J.J.ChavezMuro@tudelft.nl
M.Popov@tudelft.nl

Pedro M. Garcia-Vite
TECNM/Instituto Tecnológico de Cd. Madero,
Tamps., México
pedro.vite@itcm.edu.mx

***Abstract*— This paper presents a hybrid methodology to analyze electromagnetic transients in a photovoltaic distributed system. The methodology consists in split the system into two parts: the external zone, where the system is reduced by a dynamic equivalent obtained by the application of Balance Realization (BR) theory and the internal zone, where the system is modeled in detail and solved by a time domain technique. The methodology, that uses a predictor-corrector method to join both zones, does not need a transmission line to interconnect the systems but an element with reactive behavior to deal with the time coupling. In the first zone, the use of BR permits to obtain a new and reduced state-space description of the system that keeps the domain dynamics of the full system. The size of this system can be reduced as much as desired. Nevertheless, the resulting size is proportional to the accuracy. The BR decreases significantly the computational cost to simulate distributed networks. No restrictions are done in the internal zone where all the dynamics elements including the control if desired, can be simulated. The internal zone commonly contains non-linear or power electronic elements.**

***Index Terms*-- Balanced realization, dynamic equivalents, electromagnetic transient analysis, frequency-domain analysis, reduced-order systems, internal and external zone.**

I. INTRODUCTION

Commonly, the transmission power systems are simulated and analyzed through models that include the electromagnetic transients dynamic (EMT) and/or the electromechanically dynamic (RMS).Frequently, EMT models have been used to study fast transients which go from atmosphere discharge to the commutation of protection element in the system caused by faults. To reproduce with fidelity the behavior of the system these methods require numerical integration with small time steps. On the other hand, the RMS. models based on phasorial analysis are used when electromechanical transient phenomena is studied, this methodology commonly uses large time steps and simplifies the machines, transmission lines and other elements with equivalents.

Dynamic equivalents have been largely used in the field of power systems, above other authors, the most representative equivalents works are: Dynamic modal equivalents [1] where the system is split into two subsystems; one zone under study and several external ones. Consistent aggregation method [1] where a group of consistent generators is represented by only one generator after a perturbation study. Artificial neural networks [3] that model in a black box manner an equivalent that represents a part of the system. Frequency depended network equivalent [3] where the R, L, and C components are used to represent a network, the equivalent characterizes the system over a frequency span. In the Two-Layer equivalents [3] approach, where the system is split into two subsystems, the external system is interfaced by transmission lines that are connected to a frequency dependent equivalent known as a deep region.

The technique used here is based on the balance realization (BR) methodology. This technique is not new, in fact, in 1981 Bruce C. Moore presented this technique [4]. It took only fourth years to be implemented in power systems [5]. After, this technique was applied in the systems to reduce the frequency spectrum used to model the electrical elements [6]. Then the technique was also in blocks and structures shapes in [7]. The BR was take back for reduction in time and frequency frames with a good results [8]-[11].

The technique used here splits the system into two subsystems; the internal and external one. The external system, represented by the space state equations, is transformed to a balanced, controllable, and observable set of equations by means of the balance realization technique. With such a technique is easy to identify the most representative modes at the point of common coupling. The internal system, represented in detail, is solved by a predictor/corrector technique based on Heun's method. This provides us accurately the voltage and current signals at the point of interconnection. The accuracy depends on the size of the new balanced system.

The remaining of this paper is organized as follow: In the second section, the balance realization technique is explained in detail, as well the Heun's method. In the third Section, this methodology is presented and tested with a didactical case of study. The fourth section, the core of the paper, the proposed methodology is applied to the 2 areas Kundur case of study

"This work was supported in part by the General Director of the National Council of Science and Technology of Mexico (CONACYT)"

978-1-5386-4505-5/18/$31.00 ©2018 IEEE

[12] interconnected with a photovoltaic system (PV). The case presents the advantages of using the dynamic equivalent. At Section V, the obtained results were compared against those found by means of the commercial software PSCAD in order to validate the propose technique.

II. BALANCED REALIZATION AND HEUN BACKGROUND METHODS

The proposed technique here is based on two mature methodologies: the balance realization and the numerical Heun technique, this section briefly describes both of them separately. Any system, represented by its state spaces, can be reduced by a controllable and observable new set of state spaces applying the balance realization.

A. Balanced Realizations

In power system studies the BR approach has been implemented to find a minimal realization of the systems under study. The main purpose of this methodology is to obtain a new state-space description where the reachability and observability are diagonalized. This new set of invariant parameters can be reduced in such a way that the most representative states of the system are preserved. The methodology is applied to the external system of the system under study.

To implement the BR approach in an LTI system consider its *n*th representation given by a set of ODES

$$\dot{x} = f(x,u), \tag{1}$$

$$y = g(x,u). \tag{2}$$

It is necessary to obtain a transformation matrix T corresponding to the change of basis for the states x to get a new set of ODES asymptotically stable and internal balanced representation of the system

$$\bar{x} = Tx. \tag{3}$$

Being the LTI characterized by the space state matrix representation expressed by:

$$\boldsymbol{\dot{X}_c} = \boldsymbol{A_c X_c} + \boldsymbol{B_c U_c}\,, \tag{4}$$

$$\boldsymbol{Y_c} = \boldsymbol{C_c X_c} + \boldsymbol{D_c U_c}\,, \tag{5}$$

where, without loss of generality, D=[0].

Then, gramians of controllability and observability must be calculated. The controllability gramian can be obtained by the equation $\boldsymbol{B} \times \boldsymbol{B^T} = \boldsymbol{P} = \boldsymbol{W_c}$. Where is possible to know if the system is controllable provided that $\boldsymbol{P}$ is invertible for all $t > 0$.

Whereas the observability gramian is calculated by $\boldsymbol{B^T} \times \boldsymbol{B} = \boldsymbol{Q} = \boldsymbol{W_o}$, if the resulting matrix is nonsingular then the system will be observable. $\boldsymbol{P}$ and $\boldsymbol{Q}$ are symmetric and positive defined. Both gramians satisfy the Lyapunov equation:

$\boldsymbol{AW}_c + \boldsymbol{W}_c\boldsymbol{A}^T = -\boldsymbol{BB}^T$ and $\boldsymbol{A}^T\boldsymbol{W}_o + \boldsymbol{W}_o\boldsymbol{A} - \boldsymbol{C}^T\boldsymbol{C}$

By the Cholesky factor decomposition, it is possible to obtain an inferior triangular matrix $\boldsymbol{R}$ with all its diagonal input strictly positives $\boldsymbol{W_c} = \boldsymbol{R^T R}$. This matrix is used to obtain a diagonal matrix $\boldsymbol{\Sigma}$, in fact, this matrix contains the Hankel singular values of the system. $\boldsymbol{RQR^T} = \boldsymbol{U\Sigma^2 U'}$, where $\boldsymbol{\Sigma} = diag\{\sigma_1, \sigma_1, \dots, \sigma_1\}$ and $\boldsymbol{U}$ is a matrix with orthogonal columns.

It is also possible to obtain the Hankel singular values by the square roots of the eigenvalues of $\boldsymbol{PQ}$,

$$\sigma_i = \sqrt{\lambda_i(\boldsymbol{PQ})}. \tag{6}$$

Applying a coordinate transformation is possible obtain a transformation matrix $\boldsymbol{T}$ for which the controllability and observability gramians are equal. The $\boldsymbol{T}$ matrix is used to obtain a new set of state space equations.

$$\begin{bmatrix} \boldsymbol{T^{-1}AT} & \boldsymbol{T^{-1}B} \\ \boldsymbol{CT} & \boldsymbol{D} \end{bmatrix} = \begin{bmatrix} \boldsymbol{A}_{br} & \boldsymbol{B}_{br} \\ \boldsymbol{C}_{br} & \boldsymbol{D} \end{bmatrix}, \tag{7}$$

where, $\boldsymbol{T} = \boldsymbol{R^{-1}U\Sigma^{1/2}}$, $\boldsymbol{T^{-1}} = \boldsymbol{\Sigma^{-1/2}U'R}$ and $\boldsymbol{A}_{br}$, $\boldsymbol{B}_{br}$, and $\boldsymbol{C}_{br}$, correspond to the internal balanced system.

B. Predictor-corrector Heun method

The Heun's or modified Euler's method [13], [14] is based on the numerical integration of the definite integral $x_{Tk+1} = x_T + \int_{Tk+1}^{T} f(T, x(t))dt$ is used to solve the detailed system.

The Heun's method consists of two stages: first, a predictor or intermediate value approximation is obtained, and then the correction or the real value is obtained

$$x'_{k+1} = x_k + \Delta t f(t_k, x_k)\,, \tag{8}$$

$$x_{k+1} = x_k + \frac{\Delta t}{2}[f(t_k, y_k) + f(t_{k+1}, x'_{k+1})] \tag{9}$$

where Δt is the step of time size. This technique can deal with high discontinuities in the electrical signals from a power system by decreasing of steady numerical oscillations.

III. HIBRID PROPOSED TECHNNIQUE

The proposed technique gathers the Heun's method and the balance realization in order to obtain the behavior of the system at the PCC. This is feasible due to the new set of state space representation can be solved jointly with the part of the system which is modeled in detail in a time domain solution. The technique is explained in detail in this section where is also possible to show the technique in a flowchart diagram

First, the system under study is split into two or more subsystems. One is called the external subsystem and the other internal subsystem. The external subsystem corresponds to the part of the system where a detailed representation is not necessary. In this part, the balance realization technique is implemented. The balance system obtained from (7) has the property that by a simple reordering and truncation of the dominant modes at the PCC is possible to obtain a reduced order model [15].

$$\dot{\boldsymbol{X}}_{\boldsymbol{r}} = \boldsymbol{A}_{\boldsymbol{r}}\boldsymbol{X}_{\boldsymbol{r}} + \boldsymbol{B}_{\boldsymbol{r}}\boldsymbol{U}_{\boldsymbol{r}},$$
$$\boldsymbol{Y}_{\boldsymbol{r}} = \mathrm{C_r X_r}.$$

The reduced model is combined with the state space representation of the internal subsystem. For this part, if desired, every component is modeled in detail. Once the two space of states are combined ($\boldsymbol{A_T}$, $\boldsymbol{B_T}$, and $\boldsymbol{C_T}$) a numerical integration technique is used, for this work the Heun technique was chosen.

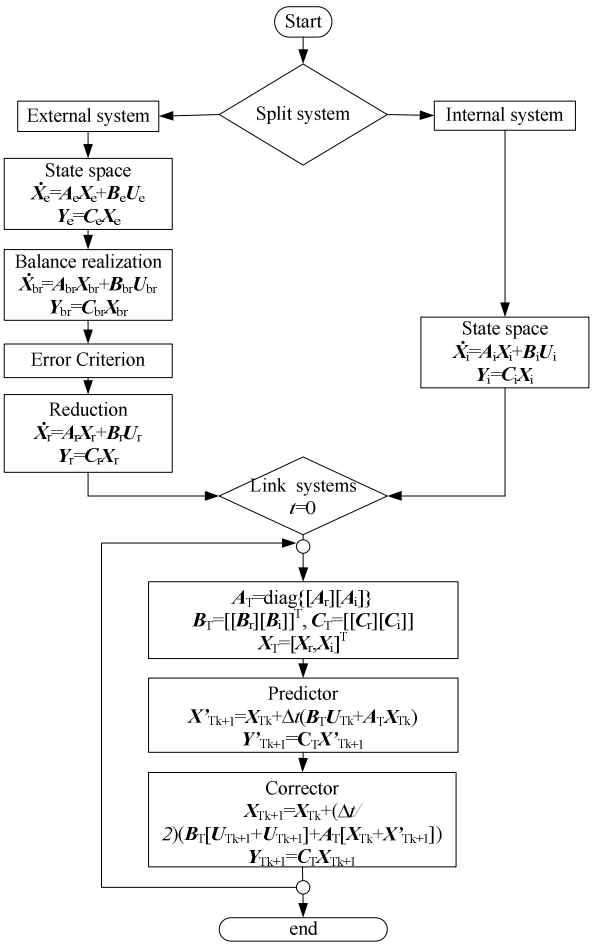

Figure 1. Dynamic equivalent technic flowchart diagram.

Fig. 1 shows a flowchart scheme of the proposed technique. Every step is followed by its respective equation. The total simulation of the system depends on the simulation time required.

The subscripts *e*, *br*, *r*, *i*, and *T* stand for the system representations: external, balance reduced, reduced, internal and total, respectively.

A. Ilustrative Example

The applicability of the proposed technique is examined in the 60 Hz system depicted in Fig. 2. The external subsystem consists of a voltage source $v_1 = 1\sin(\omega_o t)$ in series with a resistance and inductance representing the most basic generator, then a π transmission line is connected. At the other end of the line, a load composed by a resistance and inductance in parallel are connected.

The point of common coupling (PCC) depicted on the system is the place where the system is split into external and internal subsystems. The internal system is composed of a source of $v_2 = 0.9\sin(\omega_o t)$ and a *T* transmission line.

Without loss of generality, the steady state characterization of the external system is:

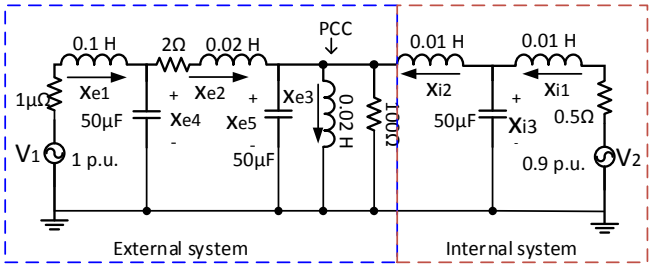

Figure 2. Illustrative example, linear system with two voltage sources.

$$\mathbf{A}_{\boldsymbol{e}} = \begin{bmatrix} -1\times10^{-5} & 0 & 0 & -10 & 0 \\ 0 & -100 & 0 & 50 & -50 \\ 0 & 0 & 0 & 0 & 50 \\ 2\times10^{4} & -2\times10^{4} & 0 & 0 & 0 \\ 0 & 2\times10^{4} & -2\times10^{4} & 0 & -2\times10^{2} \end{bmatrix},$$

whereas $\mathrm{B_e} = \begin{bmatrix} 10 & 0 & 0 & 0 & 0 \\ 0 & 0 & 0 & 0 & 20\times10^{3} \end{bmatrix}^{\mathrm{T}}$, and $\mathrm{C_e} = [0 \quad 0 \quad 0 \quad 0 \quad 1]$.

Following the procedure described in section III, the system is balanced by obtaining the Gramians and the transformation matrix.

$$\boldsymbol{T} = \begin{bmatrix} -2.7638 & -0.0627 & 0.0160 & 1.1130 & 4.0970 \\ 1.6203 & 0.1233 & -0.2513 & -6.021 & 4.1101 \\ 5.3216 & -0.1760 & -0.1534 & 3.2735 & 4.0758 \\ 2.5356 & -110.783 & -88.054 & 1.4443 & 4.5044 \\ -2.7830 & -88.0458 & 110.822 & 4.9920 & -1.8112 \end{bmatrix}$$

Using (7) the balance realization of the system is composed of the next set of matrices.

$$\boldsymbol{A}_{br} = \begin{bmatrix} -0.08491 & -808.5 & -21.46 & -0.2133 & 0.1105 \\ 808.1 & -85.52 & -126.2 & -32.15 & 3.522 \\ 20.94 & -126.2 & -191.8 & -1661 & 6.278 \\ -0.1314 & 32.11 & 1661 & -0.3932 & 0.285 \\ 0.02214 & -2.332 & -4.161 & 0.1631 & -22.22 \end{bmatrix},$$

$$\boldsymbol{B}_{br} = \begin{bmatrix} 1.382 & -0.0372 & -0.0079 & 0.5565 & 1.358 \\ -2.416 & 88.05 & 110.8 & -4.961 & 1.198 \end{bmatrix}^{\mathrm{T}},$$

and

$$\boldsymbol{C}_{br} = [\,2.783 \quad 88.05 \quad 110.8 \quad 4.992 \quad -1.811].$$

The Hankel singular values are:

$$\boldsymbol{\Sigma} = diag\{45.6067, 45.3235, 32.0194, 31.6874, 0.0738\}$$

For the internal subsystem the steady state characterization is:

$$\boldsymbol{A}_i = \begin{bmatrix} -50 & 0 & -100 \\ 0 & 0 & 100 \\ 20 \times 10^3 & -20 \times 10^3 & 0 \end{bmatrix},$$

$$\boldsymbol{B}_i = \begin{bmatrix} 90 & 0 & 0 \\ 0 & -100 & 0 \end{bmatrix}^T, \text{ and } \boldsymbol{C}_i = [0 \quad 1 \quad 0].$$

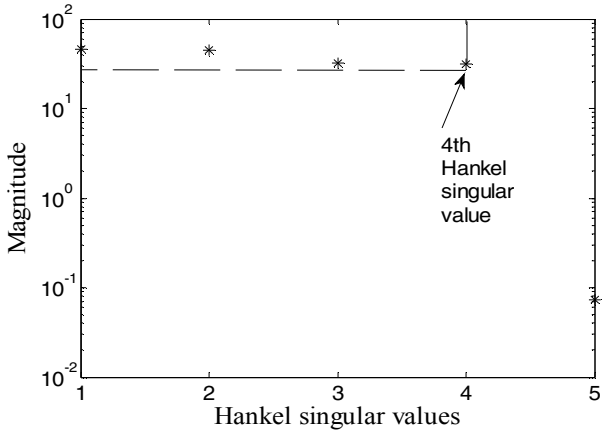

Figure 3. Illustrative example, showing the Hankel values.

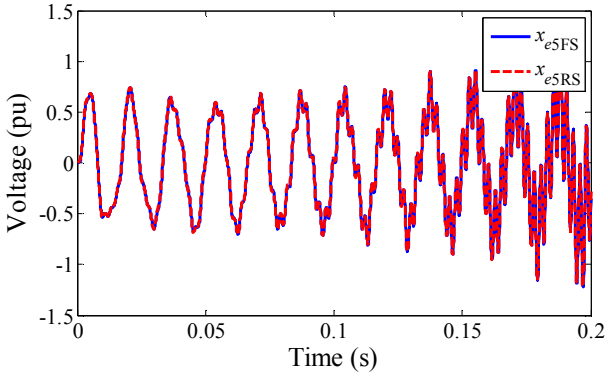

Figure 4. Comparison of voltages in the PCC between full system and the reduced system

By the analysis of the resulting Hankel values, the external subsystem can be reduced. The system cannot be reduced arbitrarily nevertheless the small Hankel values usually indicate the states that can be removed to simplify the system without losing accuracy representation. Fig. 3 shows in a semilogarithmic graphic the Hankel values for the reduction of the system; the values above 0.1 were considered with a good approximation. The system was reduced from 5 space variables to 4 (20%) with a reasonable approximation.

The voltages at the PCC x_{e5} with the full system (FS) and with the reduced system (RS) were compared in Fig. 4. The simulation starts with the sources voltage given previously for the system from Fig. 2. After 0.1s, a third harmonic distortion was injected $v_{1H} = v_1 + (0.25\sin(3\omega_0 t))$. The system was simulated during 0.2s. The current from the internal zone to the external zone is also compared in Fig. 5.

The absolute error presented with the 20% reduction is shown in Fig. 6. It can be noticed that during the first part of the simulation when there is not harmonic distortion the maximum error presented is 0.001pu and starts increasing once exists harmonic excitation at the external system. Nevertheless, the maximum error reported was 0.04pu. It is worth to say that some Hankel values are strongly linked to the PCC, these elements are the ones which has the highest magnitude (see Fig. 3). If the reduction of the system is not suitable the resulting state of spaces can be unstable.

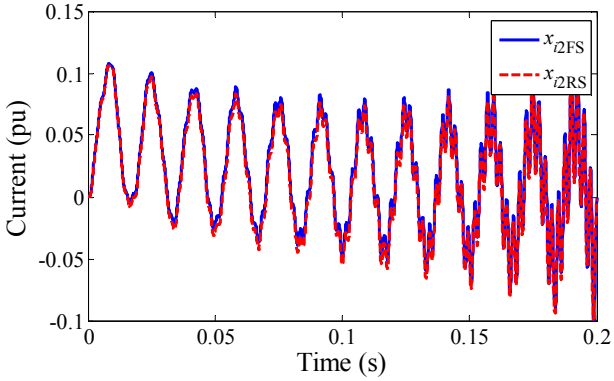

Figure 5. Comparison of currents from the internal subsystem to the external subsystem between full system and the reduced system.

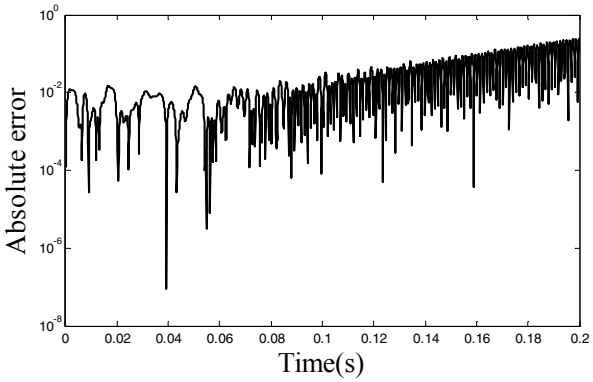

Figure 6. Logarithmic error between the full system and the reduced system.

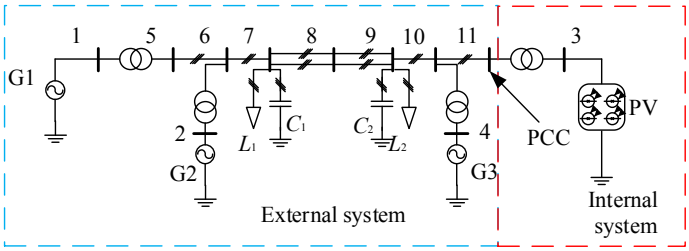

Figure 7. Case of study2, Kudor's based system with a photovoltaic distributed generator connected at bus 11.

IV. CASE OF STUDY

To prove the effectivity of the methodology, in this section a more complex system is used, the system is well known as a 2 areas Kundur's taken from [12]. A slight modification from the original work was done at bus 11 where a photovoltaic system was connected instead of a synchronous generator. The photovoltaic system including the transformer between buses 3 and 11 was considered as the internal subsystem, the rest as the external subsystem. Fig. 7 depicts the case of study where the interconnection of internal/external subsystems is

highlighted in the PCC, the parameters of the external system can be found on [12].

On Fig. 8, the photovoltaic system is presented. The filter parameters, DC link capacitance, and source values are summarized on Table I.

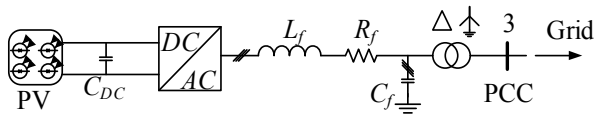

Figure 8. Internal system: photovoltaic system in a single line diagram.

TABLE I. Parameters of the photovoltaic system.

Symbol	Values	Name
PV	1.4 kV	DC voltage
PV	1.4 Ω	Resistance
C_{DC}	5 mF	DC link capacitance
L_f	0.02 H	L filter
R_f	10 Ω	R filter
C_f	100 µF	C filter

For the photovoltaic system the control is shows in Fig. 9 was implemented, only positive sequence was taken into account to control the power delivered to the system by the voltage source converter (VSC).

The Park transformation was used in order to change the reference frame from *abc* to *dq0* coordinates in this way it is possible to obtain I_{sq}^{+} and I_{sd}^{+} from I_{abc} the instantaneous current at the PCC. The resulting I_{sq}^{+} and I_{sd}^{+} signals are compared against the referent currents I_{sq}^{+*} and I_{sd}^{+*}, being the PV system balanced $I_{sq}^{+*} = 0$. After the current comparison, a PI control is used, where the PI parameters were tuning according to the system [16].

Before obtaining the modulation signals, the PI resulting parameter is added to the positive voltages. In that way is how the PV system is controlled. Modulation voltages (v_{ma}, v_{mb}, and v_{mc}) are compared against a triangular signal in order to obtain the pulses to open and close the internal VSC valves [17]. All this control is utilized to get the maximum power that the photovoltaic system can supply and thanks to that, this system can contribute to the desired real and reactive power.

The state space representation of the external system is composed of 60 spaces in that sense the matrix representation set has dimensions of $\mathbf{A}[60 \times 60]$, $\mathbf{B}[60 \times 12]$, and $\mathbf{C}[3 \times 60]$. While, for the internal system the sizes of the matrices are $\mathbf{A}[10 \times 10]$, $\mathbf{B}[10 \times 4]$, and $\mathbf{C}[3 \times 10]$.

The resulting Hankel values, which are obtained from the balanced system, were plotted on Fig. 10. The Hankel higher values represent the states that have a major influence in the PCC if this values are removed from the study system the resulting equivalent behavior will not have relation to the original system. In the same way, the smaller Hankel values have a minor influence in the system, therefore, they can be removed from the study system without losing the true behavior of the system at the PCC. However, the reduction cannot be done arbitrarily and an analytical procedure to choose the most representative Hankel values for the system is an open topic for an oncoming work. For this case of study and after several reductions test, the authors have determined to reduce the system considering only the Hankel values above 1×10^{-3}.

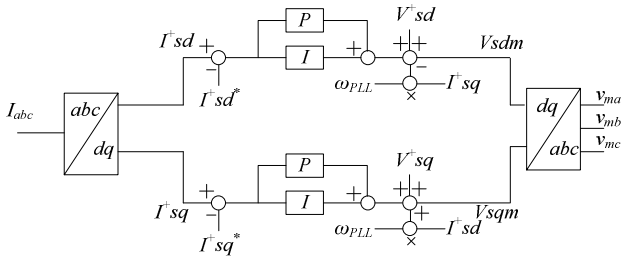

Figure 9. Internal system: photovoltaic system in a single line diagram.

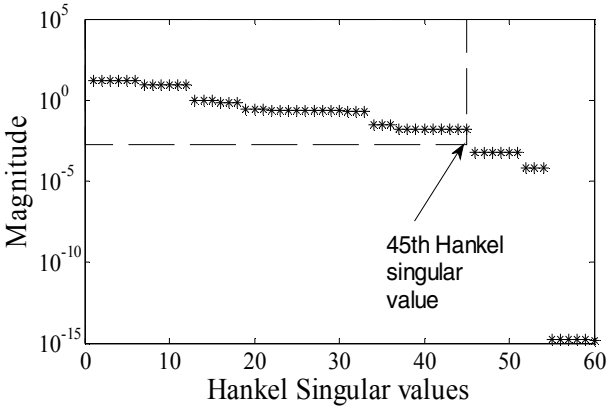

Figure 10. Hankel values of the external system.

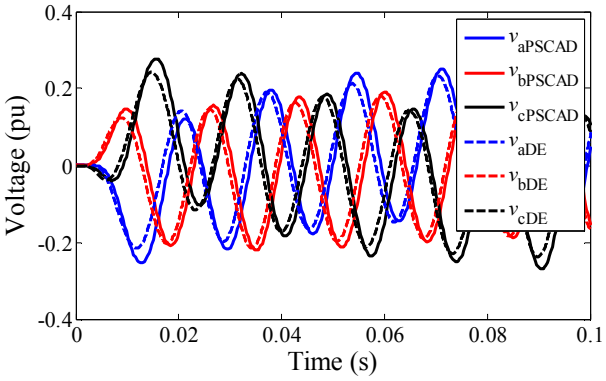

Figure 11. Voltages at the point of common coupling v_a, v_b, and v_c by Dynamic Equivalent (DE) and by PSCAD.

The system dimension was reduced by 15% of the original with a good approximation in the current and voltages, these wave shapes are shown in Fig. 11 and Fig. 12. The new set of state space representation, controllable and observable, had the dimensions of $\mathbf{A}[45 \times 45]$, $\mathbf{B}[45 \times 12]$, and $\mathbf{C}[3 \times 45]$. The simulation time decreases from 1.22s, original system, to 1.02s dynamic equivalent around 16.13%.

Once the external system is reduced, both the internal and the external subsystems can be interconnected with the hybrid technique. In Figure 11 and Figure 12 currents and voltages signals at the PCC from the dynamic equivalent (DE) and PSCAD were compared along 0.1s small difference can be seen in the signals. The step of time was set equal to $50\mu s$ for both techniques[18].

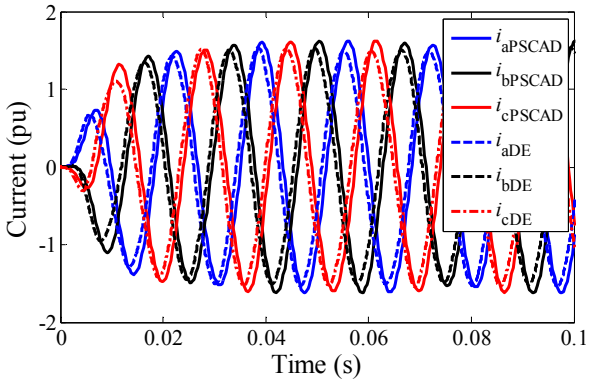

Figure 12. Currents flowing through the point of common coupling i_a, i_b, and i_c by Dynamic Equivalent (DE) and by PSCAD.

V. CONCLUSIONS

The technique presented in this paper is based on balanced realization and Heun's method. The purpose of this technique is to transform the natural state space representation of a portion of the system in a new state-space description so that the reachability and observability gramians are diagonalized and in this way, a truncation based on the new eigenvalues is effectively used. A great advantage presented by the methodology is the visual truncation decision and in accordance with the magnitude of the resulting Hankel values, the smallest values correspond to the states with a minor participation at the point of common coupling. It is worth to say that the dynamic of the system is not affected by the reduction. In parallel, the rest of the system is simulated in time-domain. The results for both techniques are gathering by a Heun numerical integration with handle the results in time-domain.

The effectiveness and feasibility of the proposed technique were tested with two systems. The first one is an illustrative example showing the steps of the methodology. It consists of a lumped parameters system representation of a generator connected to a transmission line, all the elements are taken as linear. Once the simulation is performed a 40% of reduction, in the state space representation, was possible without losing the accuracy. A second system a Kundur's modified system with a PV generator modeled to detail was simulated. The system was reduced by 15% the original size and the presented error was less than 1e-2. The reduction of the system was directly proportionally to the computational time.

The technique can easily be implemented in real time to decrees the system of system and deal with the available resources.

REFERENCES

[1]. T. Noda, "Identification of a multiphase network equivalent for electromagnetic transient calculations using partitioned frequency response," *IEEE Trans. Power Del*., vol. 20, no. 2, pt. 1, pp. 1134–1142, Apr. 2005

[2]. J. Lawler and R. A. Schlueter, "Modal-coherent equivalents derived from an RMS coherency measure", *IEEE Trans. Power Apparatus and Systems*, Vol. PAS-99, July/Aug 1980.

[3]. U. D. Annakkage *et al*., "Dynamic system equivalents: A survey of available techniques," *IEEE Trans. Power Del*., vol. 27, no.1, pp.411-420, January 2012.

[4]. B. Moore, "Principal component analysis in linear systems: controllability, observability, and model reduction", *IEEE Trans. Autom. Contr*ol, vol. AC-26, pp. 17-32, February 1981.

[5]. G. Troullinos and J. F. Dorsey, "Application of balanced realizations to power system equivalents," *IEEE Trans. Automat. Contr.*, vol, AC-30, pp. 414-416, April 1985

[6]. M. Ubaid, Al-Saggaf, and G. Franklin, "Model reduction via balanced realizations: an extension and frequency weighting techniques," *IEEE Trans. Automat. Contr*., vol. 33, pp. 687-691, July 1988.

[7]. A. Zilouchian and P. K. Agaee, "Model reduction of large scaled systems via frequency-domain balanced structures," *in Proc. of the American Control Conference*, Albuquerque, New Mexico, pp. 3873-3876, June 1997.

[8]. S. L. Varricchio, F. D. Freitas, and N. Martins, "Hybrid modal-balanced truncation method based on power system transfer function energy concepts," *IET Gener. Transm. Distrib*., 2015, Vol. 9, Iss. 11, pp. 1186–1194.

[9]. A. Ramirez, A. Mehrizi, D. Hussein, M. Matar, M. Abdel, J. J. Chavez, A. Davoudi, and S. Kamalasadan, "Application of balance realization for model-order reduction of dynamic power systems equivalents" *IEEE. Trans. Power Del.,* vol. 31, no.5, pp. 2304-2312, October 2016.

[10]. A, Ramirez, and J. J. Rico, "Harmonic/State Model-Order Reduction of Nonlinear Networks," *IEEE Tran. Power Delivery*, Vol. 31, No. 3, June 2016.

[11]. C.M. Rergis, A.R. Messina, and R.J.Betancourt, "Model-order Reduction using Truncated Modal Balanced Realization," *North American Power Symposium (NAPS),* 2015

[12]. P. Kundur, "Small-Signal Stability" in *Power system stability and control,* pp. 813

[13]. J. J. Leader, "Numerical Analysis and Scientific Computation," Pearson Education, Boston, USA 2004.

[14]. F. L. Alvarado, R. H. Lasseter, and J. J. Sanchez, "Testing of trapezoidal integration with damping for the solution of power transient problems," *IEEE Trans, on power apparatus and systems*, vol. PAS 102, pp 3783-3790, 1983

[15]. M. Orozco, "Reducción de orden a través de realizaciones balanceadas para el análisis de interconexión de un sistema fotovoltaico a la red eléctrica," M.S. thesis, TecNM-Morelia, Michoacán, México, 2017.

[16]. E. Muljadi, M. Singh, and V. Gevorgian, " PSCAD Modules Representing PV Generator," NREL, Golden, CO, 2013

[17]. M. Dahleh, M. Dahleh, and G. Verghese, "Lectures on Dynamic Systems and Control," EECS, Massachusetts Institute of Technology, Spring 2011.

[18]. N. Watson and J. Arrillaga, Power Systems Electromagnetic Transients Simulation, IET Power and Energy Series 39.